Gutenberg-Richter's law in sliding friction of gels

Tetsuo Yamaguchi,[1] Masatoshi Morishita,[1] Masao Doi,[1] Takane Hori,[2] Hide Sakaguchi,[2] and Jean-Paul Ampuero[3]

Received 4 April 2011; revised 28 September 2011; accepted 29 September 2011; published 13 December 2011.

[1] We report on experimental studies of spatio-temporally heterogeneous stick-slip motions in the sliding friction between a hard polymethyl methacrylate (PMMA, plexiglass) block and a soft poly-dimethyl siloxane (PDMS, silicone) gel plate. We perform experiments on two PDMS gels with different viscoelastic properties. For the less viscous gel, large and rapid events are preceded by an alternation of active and less active periods. For the more viscous gel, successive slow slip events take place continuously. The probability distributions of the force drop, a quantity analogous to seismic moment, obey a power law similar to Gutenberg-Richter's empirical law for the frequency-size statistics of earthquakes, and the exponents of the power law vary with the plate velocity and the viscosity of the gel. We propose a simple model to explain the dependence of the power law exponent on the plate velocity, which agrees with experimental results.

Citation: Yamaguchi, T., M. Morishita, M. Doi, T. Hori, H. Sakaguchi, and J.-P. Ampuero (2011), Gutenberg-Richter's law in sliding friction of gels, *J. Geophys. Res.*, *116*, B12306, doi:10.1029/2011JB008415.

1. Introduction

[2] Describing the spatio-temporal complexity of earthquakes is known as one of the most challenging problems to study with physics-based models due to their strong nonlinearity and large number of degrees of freedom [*Strogatz*, 1994]. However, earthquake catalogs usually show a simple power-law relationship between the magnitude and the number of earthquakes, which is known as "Gutenberg-Richter's law" (GR law) [*Gutenberg and Richter*, 1965]. Numerous attempts have been made to understand the physical origins of the complexity of earthquakes and the simple scaling of the GR law [*Scholz*, 2002]. *Burridge and Knopoff* [1967] introduced a basic model (BK model) to mimic complex sequences of earthquakes that consisted of a chain of blocks elastically coupled together and to a loading plate, and subject to velocity-dependent frictional contact with a fixed plate. At that time, the number of blocks considered in the model was quite moderate due to the limited computational resources available. Therefore, spatio-temporal complexity with a broad range of scales could not be realized. Nonetheless, owing to the velocity-dependent friction, the BK model produced highly complex stick–slip motions even with only a few blocks. As a result, further efforts were focused on developing velocity-dependent frictional constitutive relationships rather than on explaining the GR law.

[3] With the advent of the concept of self-organized criticality (SOC) [*Bak et al.*, 1987], the GR law was highlighted as a typical topic of SOC study. With the help of computer power, *Carlson and Langer* [1989] extended the BK model simulations to a larger number of blocks. They found out power-law statistics of slip events without requiring any spatial heterogeneity in their model parameters. Following their work, Olami et al. introduced a non-conservative cellular automaton model (OFC model) [*Olami et al.*, 1992; *Christensen and Olami*, 1992] that reproduced the GR law. Moreover, its exponent (called *b* value in seismology) was reported to vary with the amount of energy dissipation during the rupture events. In actual earthquake catalogs, the *b* value is significantly variable [e.g., *Mogi*, 1967; *Utsu*, 1974; *Scholz*, 2002; *Mori and Abercrombie*, 1997; *Schorlemmer et al.*, 2005], but the systematics and origins of such variability have not yet been elucidated.

[4] On the other hand, attempts to understand earthquake physics through experimental approaches have been conducted for decades. Like in the BK model during its early development stage, most of the laboratory experimental studies were aimed at establishing frictional constitutive relationships for natural faults from frictional experiments on rock or gouge samples [*Dieterich*, 1978, 1979; *Ruina*, 1983; *Marone*, 1998; *Scholz*, 1998]. However, a rock specimen for frictional tests is intrinsically not suitable to mimic the rupture process with spatio-temporal complexities to investigate the physical meaning of the GR law in earthquakes, because each rupture is too large compared to the specimen size due to the stiffness of the rock. These limitations are analogous to those of a BK model with few degrees of freedom.

[5] Unlike hard materials, soft elastic materials like rubbers or gels can produce slip events of various sizes. *Vallette and Gollub* [1993] studied the sliding friction of a thin latex membrane in contact with a translating glass rod, which is equivalent to the 1D version of the BK model. *Ciliberto and Laroche* [1994] performed friction experiments between two elastic rough surfaces. They found a power-law behavior in

[1]Department of Applied Physics, University of Tokyo, Tokyo, Japan.
[2]IFREE, JAMSTEC, Yokohama, Japan.
[3]Seismological Laboratory, California Institute of Technology, Pasadena, California, USA.

0148-0227/11/2011JB008415

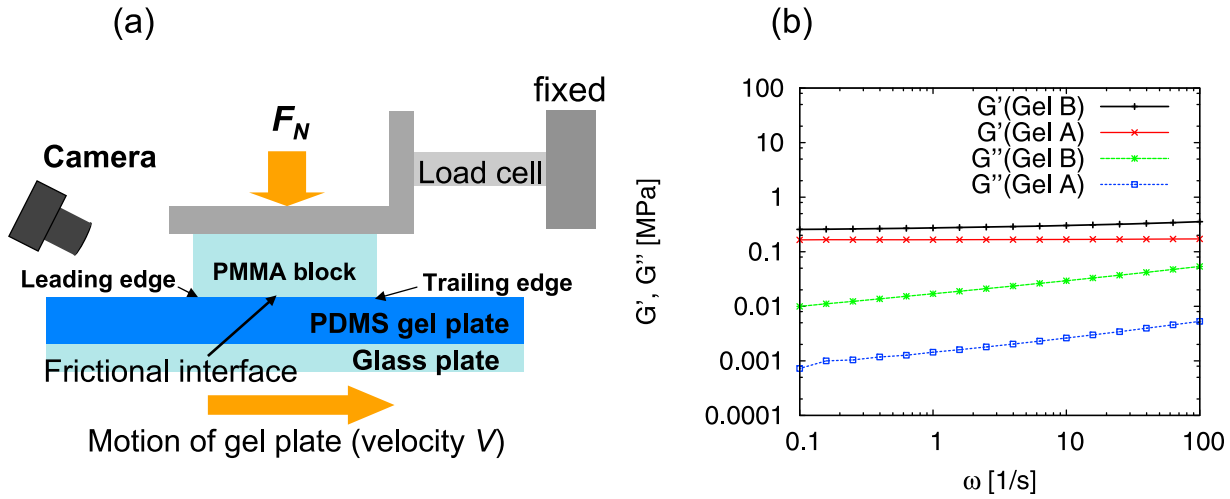

Figure 1. (a) Schematic of experimental apparatus, and (b) linear viscoelasticity $G'(\omega)$ and $G''(\omega)$ at room temperature for gel A (less viscous gel) and gel B (more viscous gel).

the statistics of slip events. Recently, the authors observed the spatio-temporal stick–slip behavior along a 2D planar interface made of an adhesive gel-sheet sliding on a glass plate [*Yamaguchi et al.*, 2009; *Morishita et al.*, 2010]. These findings suggest that soft materials such as rubbers or gels are relevant analogue materials to study spatio-temporal complexity in earthquakes.

[6] In this paper, we report on the spatio-temporally heterogeneous stick–slip motions in the sliding friction between a hard PMMA block and a soft PDMS gel plate. In order to investigate the relationship between energy dissipation and sliding behavior or slip statistics, we performed experiments using two PDMS gels having different viscoelastic properties. The details of the experimental materials and method are described in section 2. As shown in section 3, sliding behavior is quite heterogeneous in spite of no specific quenched disorder in these systems. Significant effects of viscous dissipations on the spatio-temporal frictional behavior are observed: the slip statistics clearly obeys a power law whose exponent depends on loading velocity and viscosity. We propose a simple model which explains the physical meaning of the power law exponent.

2. Experiment

2.1. Experimental Apparatus

[7] Figure 1a shows our experimental setup. A polymethyl methacrylate (PMMA) block (L = 30 mm (sliding direction), W = 100 mm (perpendicular to sliding direction), H = 20 mm (thickness)) with optically flat surface is connected to a load cell (force sensor) and is slid against a poly-dimethyl siloxane (PDMS) gel plate (L = 200 mm, W = 200 mm, H = 10 mm) prepared on a glass plate. The upper PMMA block and the load cell are fixed and the lower gel plate was driven at a constant velocity V, ranging from 1000 μm/s to 1 μm/s. A constant normal force F_N = 8.8 N was applied. The lateral force F acting on the block was measured by the load cell and represents the friction force. Sliding friction between the PMMA block and PDMS gel plate was not spatially uniform nor temporally steady, but proceeded by localized and sporadic interface detachment episodes of various sizes. It is the purpose of our experiments to image the spatio-temporal evolution of these detachment events which, by analogy to earthquakes, we will call also "slip events."

2.2. Sample

[8] Two types of PDMS gels (hereafter called gel A and gel B) were prepared. Gel A was prepared by curing a mixture of SILPOT 184 polymer: SILPOT 184 curing agent: SE 1886 A: SE 1886 B (Toray Dow Corning, Japan) = 30 : 2 : 4 : 16 in weight fraction. For gel B, PDMS polymer with a 5 wt% of curing agent (SILPOT 184, Toray Dow Corning, Japan) was used. After each prepolymer was stirred by an agitator, it was degassed by a vacuum pump to remove air bubbles, poured onto a flat glass plate with a mold, and cured at 120 deg for 3 hours. Rheological measurements were done using a rheometer (Anton Paar MCR301, parallel plate, d = 25 mm) for the above 2 samples. Figure 1b shows the results for the linear viscoelasticity at room temperature. The storage modulus (G') is almost the same for both samples ($\sim$0.2 MPa for all frequency ranges), while their loss modulus (G'') is about one-order of magnitude different, i.e., gel A has a less viscous character than gel B. Though both gels are considered to include liquid components, no solvent coming out from the gel was observed for both samples during friction experiments. It suggests that the lubrication effect is negligible in our system, unlike the gel systems reported by *Baumberger et al.* [2002, 2003] (in fact, we observed the propagation of Schallamach waves [*Schallamach*, 1971] rather than self-healing slip pulses). Due to the preparation of the gels on the glass plate, strong adhesion between the gel and the bottom glass plate was maintained during experiments without any decohesion or slippage at the bottom interface.

2.3. Visualization

[9] The spatial pattern of the slip region was observed by a simple technique shown in Figure 1a. In this setup, since a white light is illuminated in a total internal reflection condition, slip (slightly detached) regions can be visualized as dark areas, while the stuck contact regions are bright. The images were taken by a high-vision camera (HDR-SR12, SONY, Japan) at 30 frames per second.

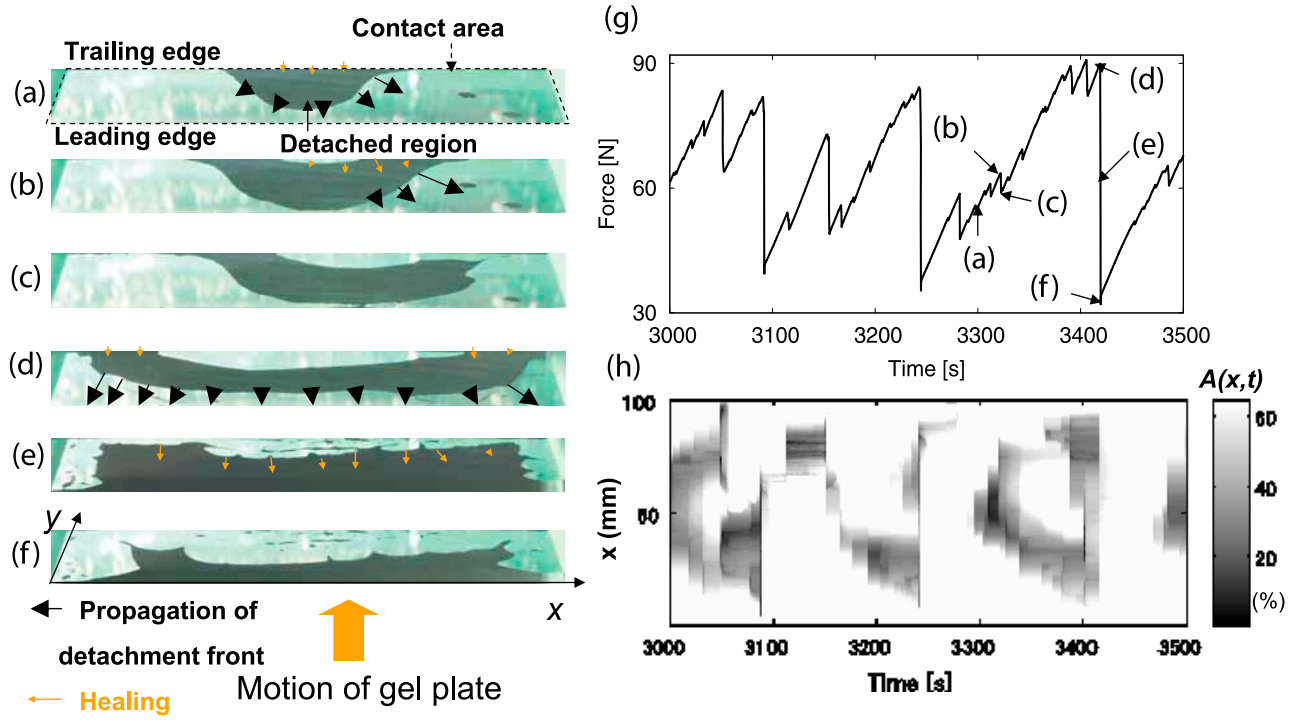

Figure 2. Slip behavior of gel A at $V = 10$ μm/s. (a–f) Representative snapshots, (g) time variation of the frictional force, and (h) time variation of the average contact area $A(x, t)$ (defined in equation (1)). The letters in Figure 2g correspond to Figures 2a–2f.

2.4. Determination of a Slip Event

[10] In this study, we represented the size of a slip event by the force drop, which is determined by the difference between the local maxima and the first subsequent local minima in the measured friction force data (see Figures 2g and 3g). With the direct use of the raw data, however, the force drop value is largely distorted due to the existence of random experimental noise (unphysical force fluctuations). Spurious local minima due to noise can "break" up a slip event before its real end or generate false small slip events when the interface is locked and there are no slip events. In order to reduce the effects of the measurement noise on the size of slip events, we discretized the measured force data by 0.05 N (several times larger than the noise level [see *Yamaguchi et al.*, 2009]) by using the "round" function. We then identified all the local maxima and the local minima in the discretized force curve $F(t)$, and defined the force drop ΔF. Even after such treatment, many false events tend to be generated at small sizes. We discarded small force drop events and adopted the slip events whose force drop values are larger than 0.1 N. As a consequence, we analyzed 145, 1407, 5089, and 9178 slip events at V = 1000, 100, 10, and 1 μm/s respectively for gel A, and 336, 1758, 8413, and 13837 events for gel B.

3. Results and Discussion

3.1. Slip Behavior

[11] Figures 2 and 3 show representative slip events at the plate velocity $V = 10$ μm/s for the two types of gel samples, gel A and gel B, respectively. Figures 2a–2f are snapshots of the spatial distribution of slip for gel A and Figure 2g shows the time variations of the friction force. The bright areas in Figures 2a–2f correspond to the contact regions, while the dark areas are the detached regions. The gap between the two surfaces in the detached regions is roughly estimated as $\sim\mu$m by the appearance of interference fringes. In Figures 2a–2f, a semi-circular detached region spreads with intermittent small events at the early stage (Figures 2a–2c), and when the region reaches some critical size (Figure 2d), a large and rapid event with a sound occurs and ruptures all the remaining areas in contact. This kind of lateral propagation behavior is characteristic of our system having a 2D frictional interface. As shown in Figure 2g, the force fluctuates during loading in the early stage (a–c) and culminates in a large force drop during the rapid detachment event (d–f).

[12] Figure 2h shows the time evolution of the contact area averaged over the y axis (parallel to the sliding direction):

$$A(x,t) = \frac{1}{L}\int_0^L A(x,y,t)dy, \qquad (1)$$

where L is the length of the block along the y (sliding) direction (x and y are indicated in Figure 2f), and $A(x, y, t)$ takes the value 100(%) if the gel is in contact with the block at (x, y) and 0 if it is detached. Thus, bright (dark) points indicate large (small) average contact areas along the y direction at a given time. Other than the spike-like patterns indicating the large and rapid propagation of detachment fronts (corresponding to large force drops in Figure 2g), small, intermittent and step-like events of the detached regions (corresponding to small force drops) were clearly observed prior to large slip events. These behaviors are

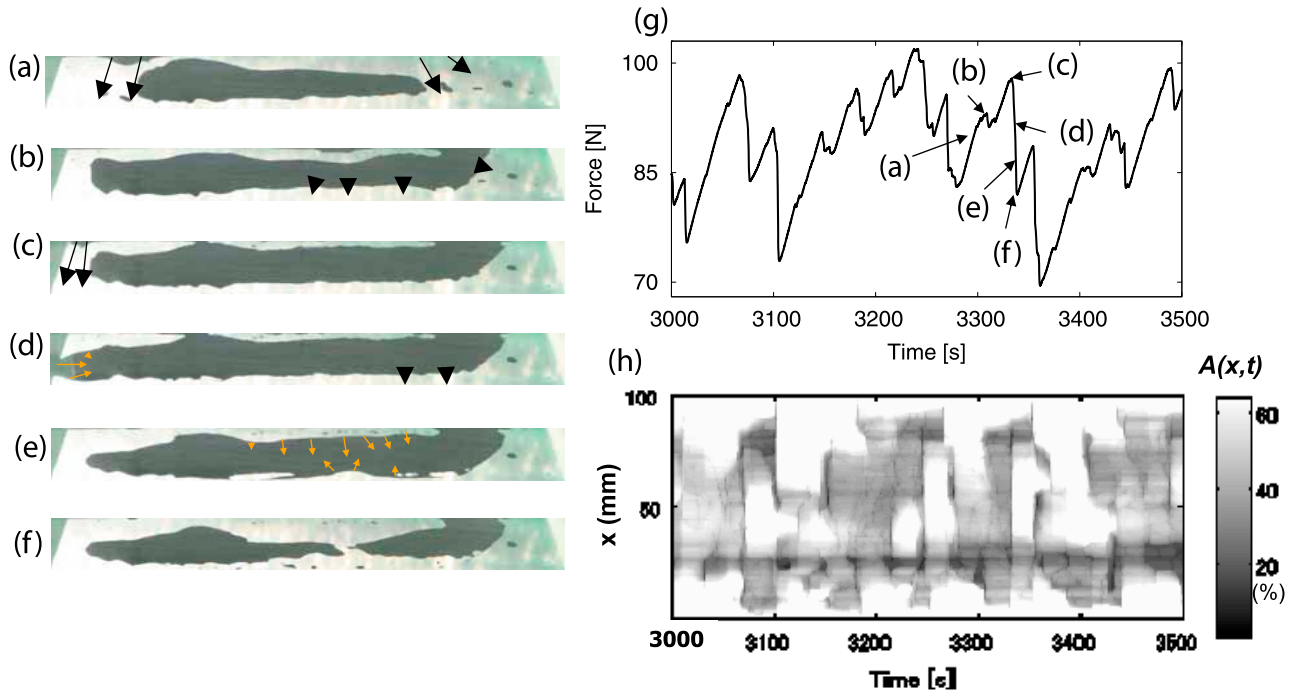

Figure 3. Slip behavior of gel B at $V = 10$ μm/s. (a–f) Representative snapshots, (g) time variation of the frictional force, and (h) time variation of the average contact area $A(x, t)$ (defined in equation (1)). The letters in Figure 3g correspond to Figures 3a–3f.

similar to those observed for the frictional system between two PMMA blocks by *Rubinstein et al.* [2004, 2006, 2007, 2008]: the onset of large frictional motion is preceded by a discrete sequence of precursor events.

[13] On the other hand, the slip behavior is different for the more viscous gel B. Figures 3a–3f show the corresponding snapshots. During shearing, the detachment fronts were slowly generated at the trailing edge and propagated towards the central region (see Figure 3a and 3b), and were accumulated to form a large detached region shown in the pictures. Then a comparatively large event ($\Delta F \sim 15$ N) took place abruptly in the left edge of the frictional interface (see Figure 3c) and stopped in the middle of the contact region. At later stages, slow healing processes were observed (small arrows in Figures 3d and 3e). During slip events in this velocity condition, there was no sound recorded by the microphone equipped on the camera, i.e., slip events in this case are considered to be "aseismic" [*Sacks et al.*, 1978; *Rogers and Dragert*, 2003; *Shelly et al.*, 2006; *Ide et al.*, 2007] (in order to confirm whether they are truly aseismic, it may be interesting to measure acoustic emissions). As is evident in Figure 3g, the force fluctuations seem irregular and

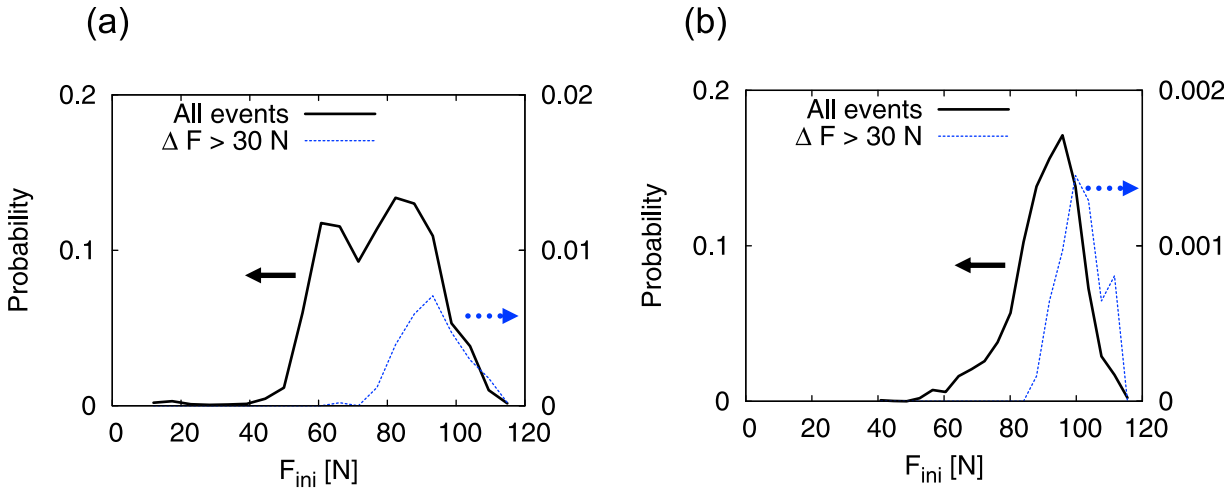

Figure 4. Probability distributions of the friction force at event initiation at $V = 10$ μm/s for (a) gel A and (b) gel B. Solid line denotes the distribution for all slip events (left axis) and dotted line for large events ($\Delta F > 30$ N, right axis). For each plot, 20 bins are used.

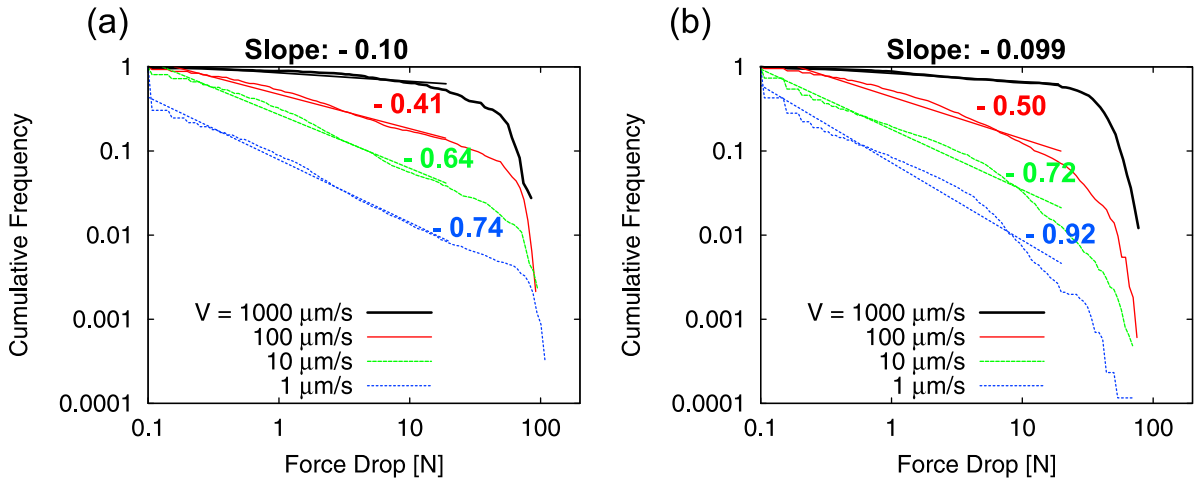

Figure 5. Cumulative frequency plots of the force drop for (a) gel A and (b) gel B at four different plate velocities. Each frequency is normalized by the total number of events. For each plot, 100 bins are used and a power-law fitting curve is also drawn.

include frequent small slip events as well as rare large events. The statistics of the event sizes are analyzed in section 3.3.

[14] Major differences between gel A and gel B appear in the spatio-temporal plots shown in Figure 2h and 3h. In gel A, a detached (dark) region nucleates and spreads in the x direction in an intermittent (step-like) manner, and abruptly disappears after a large and rapid detachment event. On the other hand, in gel B, detached regions are always present on the interface, and successive, slow detachment motions are seen.

3.2. Statistics of Force at Initiation

[15] Figure 4 shows the probability distributions of the friction force F_{ini} when a slip event is initiated. Figures 4a and 4b correspond to gel A and B respectively, and the plate velocity V is 10 μm/s in both experiments. As shown in Figure 4a for gel A, the distribution considering all slip events has a bimodal shape while the distribution considering only large events with $\Delta F > 30$ N has a single peak around 90 N. This means that, as the shear loading proceeds after a large slip event, slip becomes active at small force levels (Friction force $\sim$60 N), turns less active at larger loads ($\sim$70 N), and finally reactivates until the next large slip event occurs ($\sim$90 N). At this moment, the underlying mechanisms responsible for this three-steps precursor activity are not understood and the relationship between this and the precursor behavior reported by *Rubinstein et al.* [2004, 2006, 2007, 2008] is not clear. Detailed analysis of the temporal evolution of local stress will be reported in a separate work. On the other hand, a large difference is seen in the force level statistics for gel B as shown in Figure 4b: unlike the bimodal distribution in gel A, the distribution is unimodal with a peak around 90 N for all events, and a peak in the distribution for the large events appeared at a slightly larger force level than the peak position for all events.

3.3. Size Distribution

[16] In order to characterize statistics of the slip size, we plotted the cumulative distributions of the force drop ΔF for gel A in Figure 5a and for gel B in Figure 5b. The cumulative distribution $N(\Delta F)$ is defined by the number of events larger than ΔF divided by the total number of events we analyzed. As is seen in Figure 5, the distributions for both gels obey a power law:

$$\log_{10} N(\Delta F) = -\beta \log_{10} \frac{\Delta F}{\Delta F_{\min}}, \tag{2}$$

where β is the exponent of the power-law distribution and $\Delta F_{\min}$(=0.1 N) is the lower cutoff of the force drop. The exponents β were determined by least squares fitting of equation (2) in the interval $\Delta F = [0.1N, 20N]$. The values were 0.10 $\pm$ 0.01, 0.41 $\pm$ 0.01, 0.64 $\pm$ 0.01, and 0.74 $\pm$ 0.01 for gel A, and 0.099 $\pm$ 0.001, 0.50 $\pm$ 0.01, 0.72 $\pm$ 0.01, and 0.92 $\pm$ 0.02 for gel B at V = 1000, 100, 10, and 1 μm/s, respectively (here we applied the single-parameter power-law fitting because it is rather simple but roughly captures the physics, i.e., the relative frequency of large events and the resulting average force drop value are characterized by β, as discussed later). The results indicate that the exponent β is dependent not only on the plate velocity, but also on the viscosity of the gel. These variations in the exponent are reminiscent of the elastic parameter α in the OFC model [*Christensen and Olami*, 1992; *Olami et al.*, 1992], and their physical meaning will be discussed in section 3.5.

[17] Here it is important to note two points. First, small precursor events prior to large catastrophic events (seen in Figures 2a–2f) constitute the power-law statistics [*Carlson and Langer*, 1989; *Stirling et al.*, 1996] for gel A (see Figure 5a). Second, as shown in Figure 5b, the size distributions for gel B at small plate velocities "bend" at an intermediate force drop ($\Delta F \sim$ 5N) and the number of the large events looks smaller than those expected from the (single exponent) power-law distribution. This might be a consequence of the suppression of the dynamic frictional weakening [*Ben-Zion et al.*, 2003; *Dahmen et al.*, 2011] due to viscoelastic dissipation.

[18] Finally, let us discuss the relationship between the b value and the exponent β. Since the force drop is